CONTRIBUTION OF ANALYTICAL TECHNIQUES TO DETERMINIG THE TECHNOLOGIES USED IN THE CERAMIC MATERIALS FROM THE FORMER WORKERS HOSPITAL OF MAUDES, MADRID (SPAIN)

ELENA MERCEDES PEREZ-MONSERRAT[1], RAFAEL FORT[1], PAULA LOPEZ-ARCE[1], MONICA ALVAREZ DE BUERGO[1], MARIA JOSE VARAS-MURIEL[1,2]

[1]Instituto de Geociencias IGEO (CSIC-UCM) C/José Antonio Nováis 2. 28040 Madrid, España; empmon@geo.ucm.es, rafael.fort@csic.es, plopezar@geo.ucm.es, monica.alvarez@csic.es

[2]Departamento de Petrología y Geoquímica. Facultad Ciencias Geológicas. Universidad Complutense de Madrid. C/José Antonio Nováis 2. 28040 Madrid, España; mjvaras@geo.ucm.es

Corresponding author:

Elena Mercedes Perez-Monserrat

empmon@geo.ucm.es

Instituto de Geociencias IGEO (CSIC-UCM) C/José Antonio Nováis 2. 28040 Madrid, España

Tlf. 0034 - 913944903

Fax 0034 - 915442535

ABSTRACT

This study is focuses on the characterisation of the pastes and enamels constituents of the decorative ceramics, cladding ceramics and mosaic tiles, covering the façades and the central garden fountain of the Former Workers Hospital of Maudes at Madrid, Spain. The structural bricks of the inner fabric walls and those used at the courtyards are also studied. Both the original and restoration materials are analysed petrographically and mineralogically and the elemental composition of the enamel is determined. The major textural and compositional variations identified in the materials are mainly due to differences in the clay raw materials and additives used, as well as to the manufacturing processes, specially firing temperatures. In addition to comparing the results of the analyses conducted to the information obtained from the references consulted, the study provides unknown data on the raw materials and technologies involved in manufacturing the ceramic materials found in a heritage building.

Keywords: firing; electron microscopy; traditional ceramics; enamels; glaze

1. INTRODUCTION

Clay materials harden when heated and that process, which can be likened to the formation of metamorphic rock [1, 2], constitutes the primary characteristic of ceramic technology. The earliest references to the use of sun-dried adobe brick date back 9000 years, to Palestine. References to the origin of fired brick for construction and decorative use can be found in the earliest Egyptian, Mesopotamian and Persian civilisations. In Spain the use of brick forms largely part of the country's Muslim legacy. The tradition and importance of its ceramic industry can be attributed primarily to the abundance of suitable raw materials as well as to historic trade routes and the cultural intermingling between the Iberian Peninsula and the rest of the Mediterranean basin. When clay materials are fired, several mineral transformations take place at high temperatures and low pressure. These reactions depend mainly on the composition of the raw material, heating rate, maximum firing temperature, remaining firing time and oxidation or reduction kiln conditions [3-5]. The firing temperatures reached can be deduced from the presence or absence of certain mineral parageneses [6]. Crystalline structures progressively decompose above their stability limit and new mineral phases which may co-exist in equilibrium with the original phases are generated. According to studies published on the mineral and textural transformations taking place during high- and low-calcium content clay firing, mineralogical variability is greater during firing in calcium-rich clay [1, 7-12].

The application of enamel to fired brick can be traced back to Babylon, when the material was coated with lead and colours were highlighted over the white, opaque and glossy enamel. Enamels are composed primarily of silica, which forms the vitreous lattice; tin oxides, which act as opacifiers; and lead oxides, which lower the melting point [13-15]. Due primarily to their high cost, tin oxides have been gradually replaced with other equally opacifying materials such as titanium, zirconium and zinc oxides as well as zirconium silicate [16-18].

This study aims to compare the information available in documentary references to the experimental data obtained by characterising the materials. Moreover, the research unveils previously unknown information on the raw materials and manufacturing techniques used to produce these ceramic materials. The added value afforded is that the object of study was a declared and protected building, the Former Workers Hospital of Maudes (Madrid, Spain). This cultural asset forms part of the built and industrial heritage of a given period of the country's history. An understanding of the provenance and selection of the suitable clay raw materials and a better comprehension of the technologies deployed, entail important implications for the conservation of these materials.

1.1. Ceramic materials in the Workers Hospital of Maudes: raw materials and processing

The Former Workers Hospital (Madrid, Spain), authored by Spanish architect Antonio Palacios Ramilo (1875-1945), was erected between 1909 and 1916. Declared as a national historic-artistic monument in 1979, today it houses regional government offices and the church remains its original liturgical function. The building mainly consists of four bays arranged diagonally around a central garden with a fountain. Its mixed masonry structure consists of limestone blocks on the outside and brick on the inside. The building façades and section of the fountain are decorated with ceramic cladding, and the basin is covered with a tile mosaic (Fig. 1). Nearly all the original ceramic cladding that adorned the façades was replaced between 1984 and 1986, when the fountain mosaic was also partially repaired. On the occasion of comprehensive façade cleaning performed in 2006-2008 [19], all the ceramic materials on the façades and fountain were thoroughly restored and conserved.

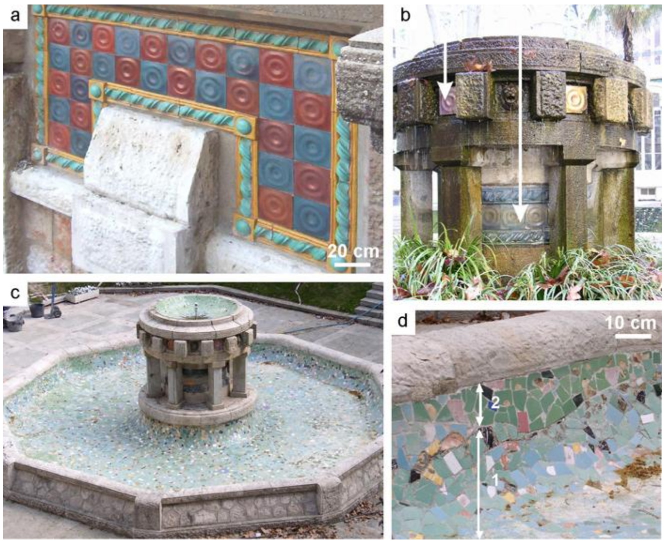

According to Perla 1990 and 2001 [20, 21], the original ceramic cladding was made by the famous ceramic artist Daniel Zuloaga in Segovia (Spain) with iron oxide-rich red clay to which silica was added; the paste was direct-fired in pinewood-fuelled kilns in an oxidising atmosphere at 1200 °C [22]; the original tile for the basin fountain was manufactured by Ramos Rejano, a company working out of Seville (Spain). Perla 1990 [20] further notes that in the nineteen eighties restoration, the ceramic cladding used to replace the original decoration was made semi-manually using clay from Madrid, and soil from Segovia, grog from Teruel and high quartz content as additives. The cladding was manufactured at Madrid in electrical kilns under oxidising conditions at

1200-1250 °C. The tiles used to repair the fountain mosaic were made from red mud, calcium-rich pastes and Madrilenian sand at Madrid's School of Ceramics, where they were fired at 1030 °C.

Zuloaga used tin, sodium and potassium to prepare the base for the enamel applied to the original ceramic cladding, to which a number of other elements were added depending on the desired colour, as well as a glazed finish; the enamel in the replacement cladding was made with a kaolin, zinc oxide, feldspar, calcite and lead base; copper and chromium oxides were added to provide green hue and it was glazed to attain a glossy finish; the enamel on the repair tiles had a lead, sodium and potassium base with lead oxide, silica and alumina [20].

2. MATERIALS AND METHODS

Table 1 and Fig. 2 contain information on the sampling and location of the decorative ceramics (enamelled ceramic cladding and tiles) and structural bricks studied, as well as the characterisation techniques used. The analyses include techniques routinely deployed in the study of ceramic materials: spectrophotometry, polarised optical microscopy (POM), X-ray diffraction (XRD) and backscattered mode scanning electron microscopy (BSE-SEM) with energy dispersive X-ray spectroscopy (EDS).

The macroscopic study covers the determination of the colour parameters of the ceramic pastes, including both the inner part of the material and its enamel. The CIELab (CIE 1986) chromatic parameters were chosen for the study, i.e., lightness (L*), which ranges from 0 for black to 100 for white, and the chromatic coordinates a* and b*. Coordinate a* ranges in value from +60 (magenta) to -60 (green) and b* from +60 (yellow) to -60 (blue). The parameters were determined with a MINOLTA CM-2002 spectrophotometer and Colour Data CM-1 software with the following measuring conditions: D_{65} CIE standard light source, 10° view angle and white tile reference.

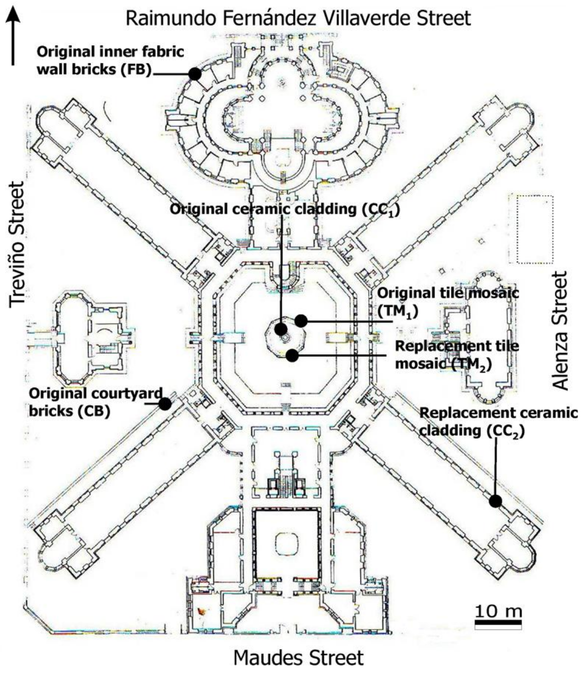

Thirty-micron thin sections of pastes and enamels were analysed petrographically by optical microscopy analysis with a polarising (transmitted light) optical microscope (POM) Olympus BX 51, fitted with an Olympus DP 12 (6V/2.5Å) digital camera. The main mineral phases in the ceramic pastes were determined on bulk samples by XRD, with the diffractometer Phillips PW-1752 and Automated Power Diffraction PC-APD [Q1] software. The instrumental conditions were 40 kV and 30 mÅ operating power, anode of copper and graphite monochromator. The measuring range was 2-68° and the recording rate 2°/min in continuous mode. The analytical software Diffract AT version EVA V 3.2 has been deployed for mineral identification.

The enamelled decorative ceramic samples were also characterised by SEM with energy-dispersive X-ray spectroscopy (EDS). The electronic scanning microscope was a JEOL JSM 6400 and the analyses conditions were 0.2-40 kV accelerating voltage, 6×10^{-10} A current, 10^{-5} Torr vacuum, 35 Å resolution, 8 mm and 35 kV working distance and 20 kV accelerating voltage for image acquisition. The spectrometer was a microanalyser Oxford instruments analytical Inca with a 133 eV-5.39 kV nominal resolution. Samples have been studied in polished graphite-evaporated thin sections, in backscattering electron mode (SEM-BSE), focussing primary the enamel thickness and its contact with ceramic paste.

The elemental composition of the enamels was qualitatively determined by means of EDS microanalyses, carrying out zone analyses. Based on the determined composition, linear elemental analyses were conducted to establish the linear distribution of the elements in the paste and enamel. Lastly, the percentage by weight (standardised) of the chemical elements comprising the main enamel components, whose atomic number determined their higher or lower contrast on SEM-BSE micrographs, was determined by means of semi-quantitative (point or zone) analyses.

3. RESULTS AND DISCUSSION

3.1. Macroscopic description

The ceramic pastes in the original ceramic cladding (Fig. 3.1a) exhibit a reddish hue (L*=67.4; a*=3.8; b*=21.7) and generous amounts of dark red putties. These pastes are much rougher than the reddish-brown (L* =66.6; a* =20.7; b* =27.1) replacement cladding (Fig. 3.2a). The paste in the tiles is homogenous (Fig. 3.3a), the original material has a peach-like colour (L* =73.3; a* =9.9; b* =20.2) and the repair tiles displays a yellowish hue (L* =75.8; a* =5.4; b* =23.2) (Fig. 3.4a).

The inner fabric wall bricks prove to be insufficiently pressed and show irregular chromatism (Fig. 3.5a). The reddish tone around the edges (L* =47.4; a* =15.4; b* =17.9) grows lighter toward the centre (L* =46.0; a* =16.7; b* =23.4), where very dark stains are observed (L*=41.3; a* =7.6; b* =12.5). The carefully manufactured and sized courtyards bricks are highly compact (Fig. 3.6a). Their light yellow hue (L* =73.0; a* =9.00; b* =26.5) is speckled by the reddish putties uniformly distributed across their surface.

The enamel applied by Zuloaga to the original ceramic cladding (Fig. 3.1a) is bluish (L* =63.1; a* =-10.2; b* =-3.2). The one applied on the replacement cladding (Fig. 3.2.a) has a bluish-green hue (L* =56.4; a* =-19.7; b* =-3.5). The enamel on the original tiles (Fig. 3.3a) is greenish-blue (L* =61.4; a* =-11.3; b* =-3.0) and green (L* =52.6; a* =-14.9; b* =17.4) in the repair material (Fig. 3.4a). The chromatic parameters determined in pastes and enamels are listed in Tables 2 and 3 respectively.

3.2. Polarised optical microscopy analyses

3.2.1. Ceramic pastes

In both the original and replacement ceramic cladding (Fig.s 3.1 and 3.2), the aggregate:paste ratio is 3:1. The aggregate consist of monocrystalline quartz grains, confirming that silica was added to the original pastes and Segovian soil to the replacement material [20], primarily as a degreaser to improve the mechanical properties of the pastes [23]. Substantial quantities of opaque minerals, possibly iron oxides, are seen. Grog, added to enhance paste strength and to avoid contraction during firing [15], and clay pellets, an indication that the paste had not been thoroughly mixed, are identified in the original cladding. The even texture observed in the replacement cladding, in terms of aggregate size and shape and of its orientation parallel or sub-parallel to the outer surface, is mainly due to the partially mechanised manufacturing procedure used [20], in which the paste was very likely extruded.

In the original tiles (Fig.s 3.3 and 3.4) the aggregate:paste ratio is 1:3 and 3:1 in the repair material (in both aggregate is also a monocrystalline quartz). This indicates that stronger pastes were employed in the restoration material. In the original tiles, the paste gets darker near the surface, primarily because the area was exposed to greater heat as a result of double firing (first the paste and then the enamel). The paste in the repair tiles has a ferruginous stain throughout, which may have been caused by the presence of iron oxides or gels "inherited" from the clay raw material [24].

The aggregate:paste ratio in the inner fabric wall bricks (Fig. 3.5) is estimated to be 1:2. Again, the aggregate comprise monocrystalline quartz grains. The variability in colour, also observed under optical microscopy, denotes firing in uncontrolled atmospheres and/or the presence of organic matter in the clay, which favoured the generation of reducing conditions inside the brick, leading to dark stains at the core [5]. The insufficient pressing was largely due to the artisanal manufacturing process, possibly at brickworks once located near the former hospital [25] with clay quarried in the surrounds. The aggregate:paste ratio in the courtyards bricks (Fig. 3.6) is estimated to be 1:4, with monocrystalline quartz aggregate. The differences in hue are mainly the result of the addition of generous amounts of grog, which made the pastes highly refractory. The cracks were caused by shrinkage around the grog, which contracted as the paste cooled. The main petrographic features observed with POM in ceramic pastes are summarized in Table 2.

3.2.2. Enamels

The enamel analysed in the original ceramic cladding (Fig. 3.1) is dark and dense and it shows gas bubbles in its interior. The thin outer layer observed may have been the result of glazing [20]. The enamel in the replacement cladding (Fig. 3.2) is lighter and the glaze that was purportedly applied [20] is not visible.

The lightly coloured enamels coating the tiles (Figs. 3.3 and 3.4) exhibit a rough surface, internal gas bubbles and numerous particles, some of which are quartz grains. The thin colourless outer layer observed in the original tiles could reveal that they may have likewise been glazed. The main petrographic features observed in the enamels studied are shown in Table 3.

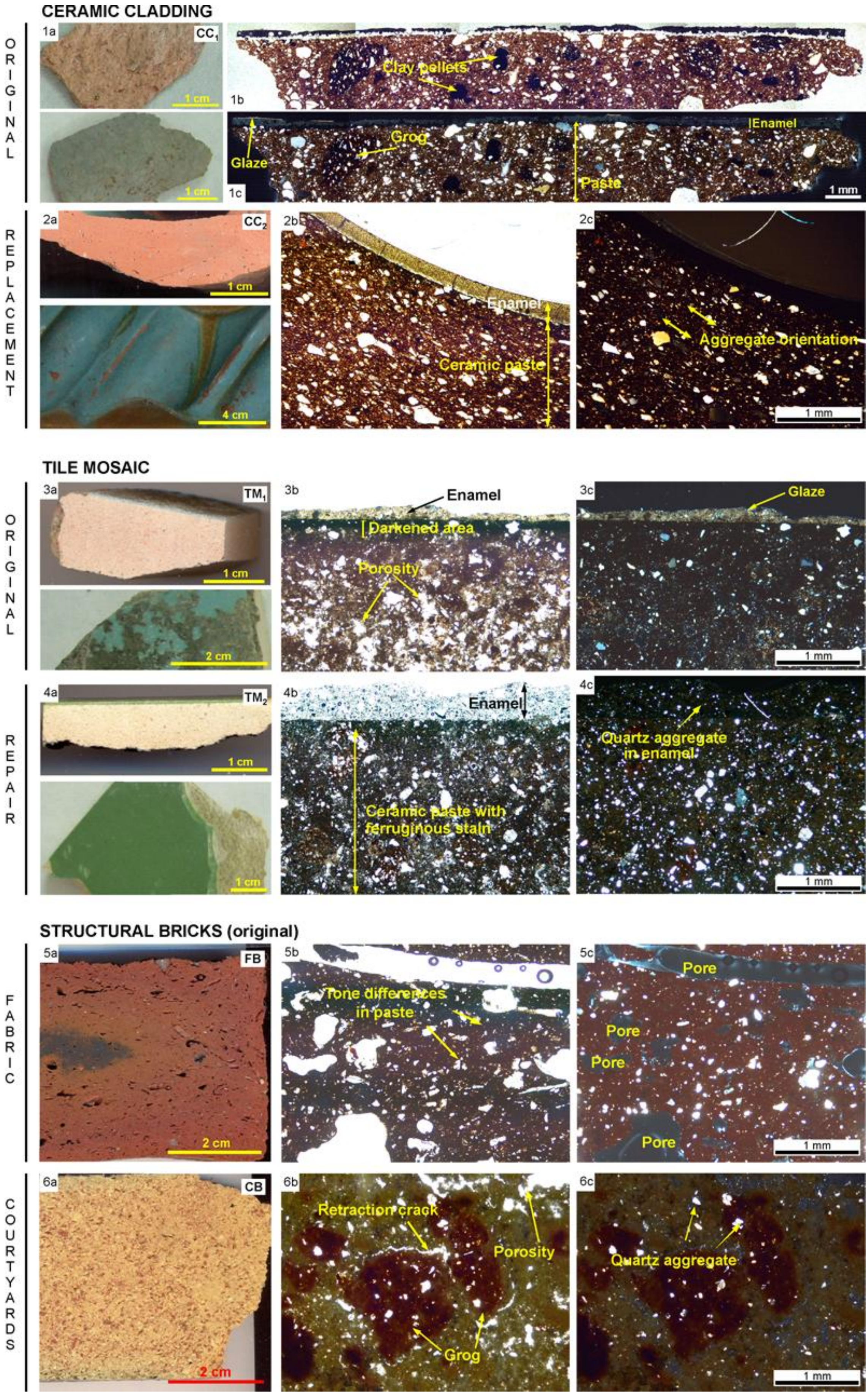
CERAMIC CLADDING
ORIGINAL
1a
CC1
1 cm
1 cm
1b
Clay pellets
1c
Grog
Glaze
Enamel
Paste
1 mm
REPLACEMENT
2a
CC2
1 cm
4 cm
2b
Enamel
Ceramic paste
2c
Aggregate orientation
1 mm
TILE MOSAIC
ORIGINAL
3a
TM1
1 cm
2 cm
3b
Enamel
Darkened area
Porosity
3c
Glaze
1 mm
REPAIR
4a
TM2
1 cm
1 cm
4b
Enamel
Ceramic paste with ferruginous stain
4c
Quartz aggregate in enamel
1 mm
STRUCTURAL BRICKS (original)
FABRIC
5a
FB
2 cm
5b
Tone differences in paste
5c
Pore
Pore
Pore
Pore
1 mm
COURTYARDS
6a
CB
2 cm
6b
Retraction crack
Porosity
Grog
6c
Quartz aggregate
1 mm

XRD analyses

The XRD analyses of ceramic pastes confirm the aggregate mineralogy recognized by polarised optical microscopy. The main mineral phases in the pastes have been identified, helping to estimate the firing temperatures based on the mineral parageneses observed (Fig. 4). The mineral phases identified are listed in Table 2.

Quartz (α–quartz) is detected in the ceramic cladding, as well as phyllosilicates in the replacement material. Although no iron compound is identified in the fractions analysed, the references consulted, the visible colour of the pastes and the opaque minerals observed with POM hinted strongly at their presence. Their existence in the material should not therefore be excluded, for if they adopted the form of micro- or nano-crystalline iron gels or are scantly present in the fractions analysed, they would not have been detected by the diffractometer used. The firing temperatures cited by Rubio-Celada 2004 [22] (1200 °C for the original pastes) and Perla 1990 [20] (1200-1250 °C for the replacement material) could not be confirmed, for the fractions analysed contained no or no identifiable mineral phases that would reveal high firing temperatures. The high quartz content identified in the original cladding ruled out such firing temperatures of 1200 °C in the fraction analysed, since quartz concentration declines drastically from 1100 °C [12]. Nonetheless, depending on their position in the kiln, some of the individual pieces may well have reached that temperature.

The mineral phases identified in both the original and replacement tile pastes include quartz (α quartz), hematite, gehlenite, diopside and wollastonite. Anorthite is also detected in the original material. The courtyards bricks pastes are observed to contain quartz (α quartz), microcline, anorthite, wollastonite and gehlenite. The presence of wollastonite (calcium silicate, $CaSiO_3$), gehlenite (calcium aluminosilicate, $Ca_2Al_2SiO_7$) and diopside (magnesium and calcium silicate, $CaMgSi_2O_6$) denotes the use of clay materials rich in calcium or magnesium carbonate [1, 12, 26], which begin to melt at lower temperatures than clay with low magnesium or calcium contents, as these elements act as fluxes [27, 28].

These high temperature (≈800-1000 °C) or neoformation mineral phases were generated in the clay paste during firing when the phyllosilicates in the clay raw material reacted with the calcium (CaO) or magnesium (MgO) oxide released during calcite ($CaCO_3$) or dolomite ($MgCa(CO_3)_2$) decomposition [10, 29, 30], following the next reactions:

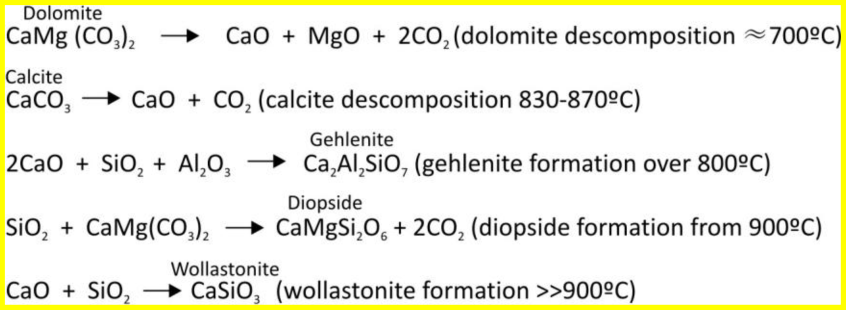

$$\overset{\text{Dolomite}}{CaMg(CO_3)_2} \longrightarrow CaO + MgO + 2CO_2 \text{ (dolomite descomposition } \approx 700\text{ºC)}$$

$$\overset{\text{Calcite}}{CaCO_3} \longrightarrow CaO + CO_2 \text{ (calcite descomposition 830-870ºC)}$$

$$2CaO + SiO_2 + Al_2O_3 \longrightarrow \overset{\text{Gehlenite}}{Ca_2Al_2SiO_7} \text{ (gehlenite formation over 800ºC)}$$

$$SiO_2 + CaMg(CO_3)_2 \longrightarrow \overset{\text{Diopside}}{CaMgSi_2O_6} + 2CO_2 \text{ (diopside formation from 900ºC)}$$

$$CaO + SiO_2 \longrightarrow \overset{\text{Wollastonite}}{CaSiO_3} \text{ (wollastonite formation >>900ºC)}$$

Gehlenite begins to form at 800 °C and to disappear at 900 °C [31] and its concentration begins to decline at temperatures of over 1000 °C; diopside and wollastonite also start to appear at 800 °C, albeit at very low concentrations [10]. The presence of gehlenite and diopside together denotes firing temperatures of over 900 °C, gehlenite alone is indicative of temperatures of over 800 °C [30] and much higher than 900 °C if wollastonite is generated [10]. Diopside forms at higher temperatures than gehlenite and its presence entails the partial disappearance of the latter [32]. Gehlenite and wollastonite are regarded as intermediate compounds [9, 33] that became unstable phases in the presence of silica and high temperatures, generating neoformation phases with a higher silica content such as anorthite (calcium aluminosilicate, $CaAl_2Si2O_8$)[1, 10, 12] according the reactions:

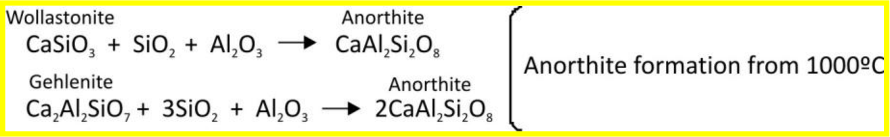

$$\left.\begin{array}{l} \overset{\text{Wollastonite}}{CaSiO_3} + SiO_2 + Al_2O_3 \longrightarrow \overset{\text{Anorthite}}{CaAl_2Si_2O_8} \\ \overset{\text{Gehlenite}}{Ca_2Al_2SiO_7} + 3SiO_2 + Al_2O_3 \longrightarrow \overset{\text{Anorthite}}{2CaAl_2Si_2O_8} \end{array}\right\} \text{Anorthite formation from 1000ºC}$$

Their presence implies that equilibrium was not reached during firing and the reactions were not carried through to completion [34]. In ceramic pastes made with calcium-rich clay, anorthite begins to form from 1000 °C [1, 10, 26].

In the ceramic paste used in the tiles and courtyards bricks, the presence of wollastonite, gehlenite, anorthite and/or diopside reveals that the clay raw material had a high calcium and/or moderate magnesium content. At longer firing times, the reactions leading to the formation of these high temperature phases would be more complete [4], since firing time controls kinetic reactions very tightly. The absence of phyllosilicates and carbonates and the presence of the aforementioned neoformation phases denote, on the one hand, that the firing temperatures used for the original tiles and courtyards bricks must have been higher than 900 °C [1, 26, 29, 30]. On the other, those results may confirm that the repair tiles were made with calcium-rich pastes and that the firing temperature was 1030 °C, as reported by [20]. The no identification of anorthite and the presence of gehlenite and wollastonite in the repair tile pastes might be attributed to a low calcium or silica content in the clay material used in their manufacture [9].

The intensity of the main diffraction peaks of the high temperature mineral phases (wollastonite, gehlenite and diopside, as well as anorthite in the original tiles and courtyards bricks) identified in the tiles and courtyards bricks may serve as grounds for establishing differences in the firing temperatures reached. The maximum diffraction peaks for diopside and wollastonite in the repair tiles and courtyards bricks would indicate higher firing temperatures than the ones reached in the original tiles. The greater intensity of the gehlenite main peaks would signify lower firing temperatures, declining Bragg peaks intensity as function of rising temperature.

The original tile pastes (Ge > Di, Wo and An) were therefore fired at a lower temperature (>800 °C) than the repair tile pastes (Ge ≈ Di and Wo; >>900 °C), which were in turn fired at lower temperatures than the courtyards bricks (Ge < Di, Wo and An; >1000 °C). Taking into account that these bricks were placed outdoors, the objective sought with these higher temperatures would have been to ensure that the material was highly refractory. The high temperature mineral paragenesis identified in the courtyards bricks (large amounts of wollastonite, diopside and anorthite and the near absence of gehlenite) reveals the use of a technology able to reach temperatures of over 1000 °C.

Furthermore, the presence of hematite generally denotes an abundance of iron oxides in the clay raw material. However, iron-rich minerals may also be generated during firing, because when clay pastes are fired in an oxidising atmosphere their iron oxides may generate in turn hematite crystals [35]. The identification of hematite in the tile pastes would support the presence of iron oxides in the calcareous clay used as raw material, since the calcareous lumps in calcium-rich clay prevent iron fixation in the network of neoformed calcareous silicate and aluminosilicate lattices and consequently inhibit the nucleation of new hematite crystals [36]. In the repair tiles, these oxides may have been present in the calcium-rich pastes used, reported by Perla 2001 [20], although the red mud used [20] was a more likely origin. The reddish hue attributed to the large amounts of grog added in the courtyards bricks may have been a result of the high iron oxide content in that constituent. Nevertheless, no iron compound has been identified in the fraction analysed, perhaps for the same reason as discussed in the case of the ceramic cladding.

The analysis of the intermediate area of the paste in the inner fabric wall bricks identifies quartz (α quartz), hematite, gehlenite and anorthite. Based primarily on the colour of these bricks, the presence of hematite would reveal the existence of iron oxides in the clay raw material, although they may have also been generated during firing according with Nodari et al. 2007 [35]. The identification of gehlenite and anorthite would denote the use of a mix of kaolinitic and calcitic clays, in which, during the firing process, metakaolinite-gehlenite-anorthite recrystallisation would have taken place, under the reactions:

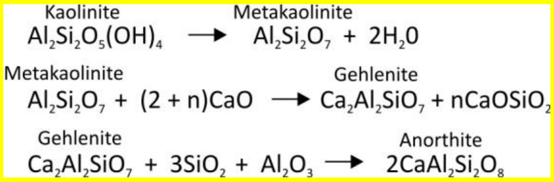

$$\underset{\text{Kaolinite}}{Al_2Si_2O_5(OH)_4} \longrightarrow \underset{\text{Metakaolinite}}{Al_2Si_2O_7} + 2H_20$$

$$\underset{\text{Metakaolinite}}{Al_2Si_2O_7} + (2+n)CaO \longrightarrow \underset{\text{Gehlenite}}{Ca_2Al_2SiO_7} + nCaOSiO_2$$

$$\underset{\text{Gehlenite}}{Ca_2Al_2SiO_7} + 3SiO_2 + Al_2O_3 \longrightarrow \underset{\text{Anorthite}}{2CaAl_2Si_2O_8}$$

These reactions would have been largely enhanced by the structural similarity among these three mineral phases and expedited by the replacement of the aluminium in the kaolinite with iron [37, 38]. The presence of gehlenite and anorthite would indicate that the temperature reached in the intermediate area of the inner fabric wall bricks must have been over 950 °C.

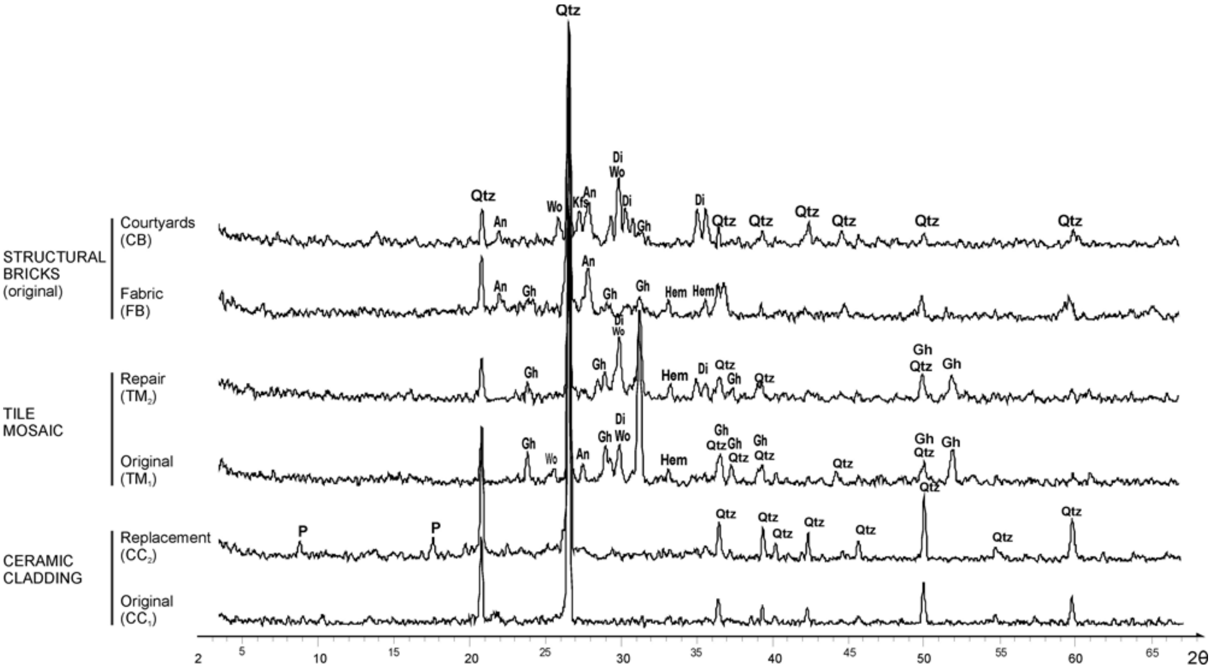

3.3. BSE mode SEM-EDS analyses

The contact between the enamel and the paste in the original ceramic cladding is continuous but snarled (Fig. 5a). The 200-μm thick layer of enamel adapts to the rough ceramic surface. Its texture is found to be highly uneven and to contain circular gas bubbles measuring an average 100 μm in diameter. The irregular paste-enamel contact and textural unevenness of the enamel are attributed largely to its manual preparation and application. The elements identified in the enamel are Al, Si, K, V, Fe, Zr and Pb. The linear distribution shows that the majority elements in the enamel are Zr and Pb. No Sn has been detected in any of the analyses carried out and titanium determined semi-quantitatively (2 and 5 point analyses at Fig. 5a) is possibly a sign that titanium oxides were used in place of their tin counterparts. The addition of Na and K [20] was confirmed. Particles with a significant V content, which may have been added for colour, are seen. Although this element also acts as a flux, it could form part of a pigment known as Zr-V blue [39], which might likewise have been the origin of the zirconium identified. The linear distribution of Fe element confirms the existence of iron oxides in the ceramic paste. The glaze applied to the enamel is a constant 20 μm thick and the contact between the two is very smooth. It consists nearly entirely of Ca (84.2 wt% in the area analysed), which reduces lead solubility and enhances gloss [13].

The contact between the enamel and the ceramic paste in the replacement cladding is smooth and continuous (Fig. 5b). No gas bubbles are observed in this uniform layer, which was a constant 500 μm thick, except around the curves where it is thicker to adapt to the shape of the piece. These characteristics denote a certain degree of mechanisation in the manufacture and application of the enamel analysed. No glaze whatsoever has been seen in the area analysed. The EDS spectrum for that area reveals the presence of Na, Al, Si, Ca, Fe, Cu, Zn, Sn and Pb in the enamel. The linear analysis shows that Ca, Cu, Zn, Sn and Pb are the main elemental constituents. The bluish green colour is largely the result of the presence of copper or iron oxides. The Na, K and Ca detected probably forms part of the feldspars, kaolin and calcite used to prepare the enamel [20]. The Pb content is lower than in the enamel covering the original cladding and the opacifying capacity afforded by tin [16] may have been partially replaced or reinforced by adding zinc oxides [18]. The high content of Sb detected should be highlighted (19.4 wt% in the area analysed) and may also have been added as an opacifying agent [39]. The relatively large amount of Cl, 6.9 wt%, may have been the result of including sodium chloride for the fluxing effect provided by Na [40, 41].

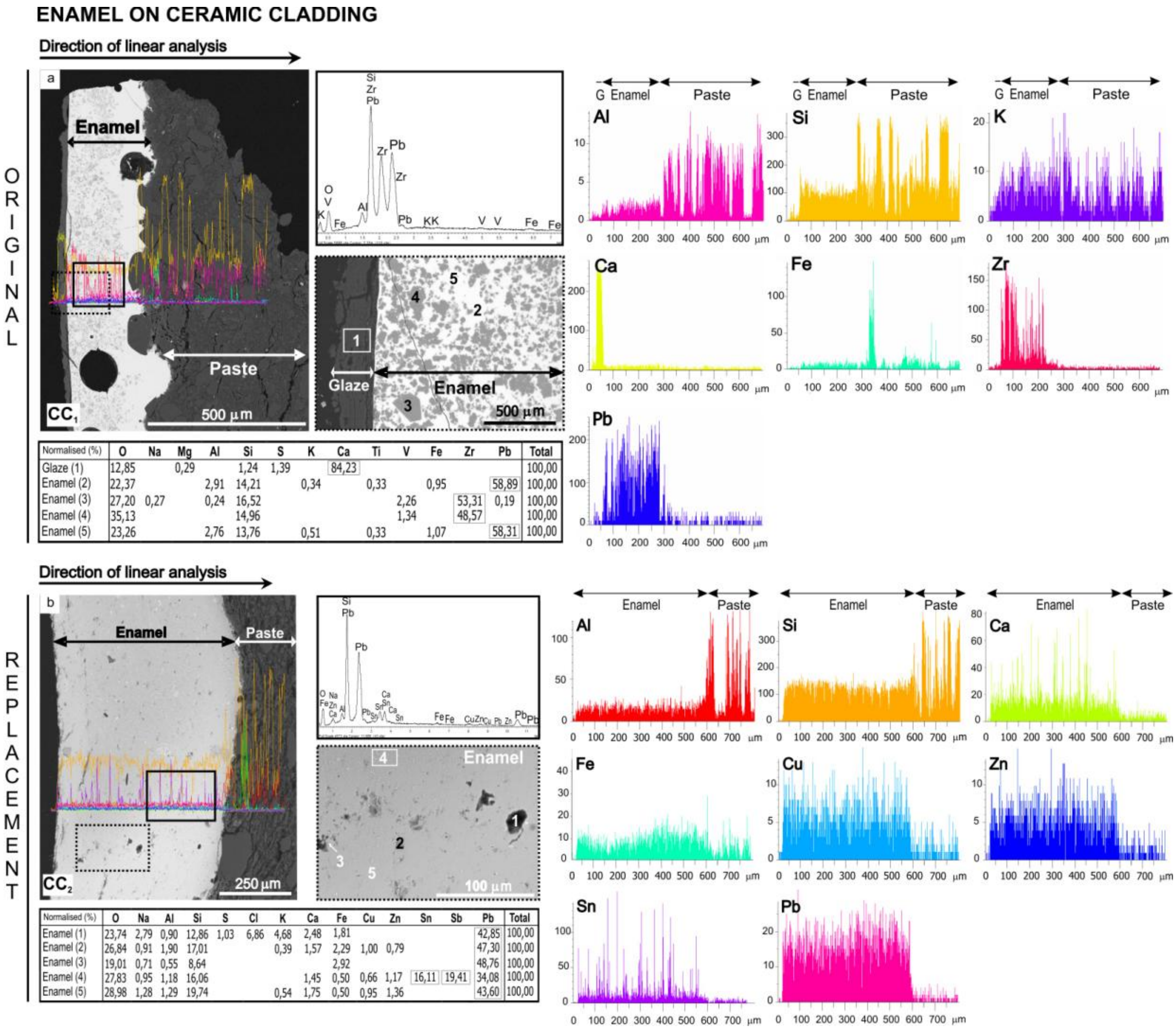

Normalised (%)	O	Na	Mg	Al	Si	S	K	Ca	Ti	V	Fe	Zr	Pb	Total
Glaze (1)	12,85		0,29		1,24	1,39		84,23						100,00
Enamel (2)	22,37			2,91	14,21		0,34		0,33		0,95		58,89	100,00
Enamel (3)	27,20	0,27		0,24	16,52					2,26		53,31	0,19	100,00
Enamel (4)	35,13				14,96					1,34		48,57		100,00
Enamel (5)	23,26			2,76	13,76		0,51		0,33		1,07		58,31	100,00

Normalised (%)	O	Na	Al	Si	S	Cl	K	Ca	Fe	Cu	Zn	Sn	Sb	Pb	Total
Enamel (1)	23,74	2,79	0,90	12,86	1,03	6,86	4,68	2,48	1,81					42,85	100,00
Enamel (2)	26,84	0,91	1,90	17,01			0,39	1,57	2,29	1,00	0,79			47,30	100,00
Enamel (3)	19,01	0,71	0,55	8,64					2,92					48,76	100,00
Enamel (4)	27,83	0,95	1,18	16,06				1,45	0,50	0,66	1,17	16,11	19,41	34,08	100,00
Enamel (5)	28,98	1,28	1,29	19,74			0,54	1,75	0,50	0,95	1,36			43,60	100,00

The enamel applied to the original tiles (Fig. 6a) is non-uniform and it has a constant 330 µm thick, approximately. Its contact with the ceramic paste is continuous although slightly snarled. It exhibits circular internal gas bubbles of various sizes, some up to 150 µm in diameter. The elements detected have been Na, Al, Si, K Ca and Pb. Si, K and Pb are the most abundant elements. The Al and K contents are particularly significant in some of the constituents of the enamel analysed. The Si forms part of some of the particles identified under the optical microscope (Fig. 3.3c). None of the elements that may have given the enamel its greenish-blue hue have been detected, no was any glaze observed.

The enamel in the repair tiles (Fig. 6b) resembles the enamel applied to the original materials very closely. Its texture is uneven and it has circular gas bubbles of different sizes (25-90 µm in diameter). Its thickness is a very constant ±450 µm, the paste-enamel contact is essentially smooth although quite uneven. The EDS spectrum reveals the presence of Na, Mg, Al, Si, K, Ca, Cl and Pb in the enamel. Here also, Si, K and Pb are the majority elements. Some of the enamel constituents have significant Al and K contents. High proportion of Ca and As particles are observed, probably added to attain respectively a glossy finish and opacify the enamel [39]. All the elements reported by [20] have been detected: Pb, Na, K, Si and Al. Chromium, added in the form of chromium oxide, was primarily responsible for the green hue [39], although the small amount of Fe detected might have also contributed.

ENAMEL ON TILE MOSAIC

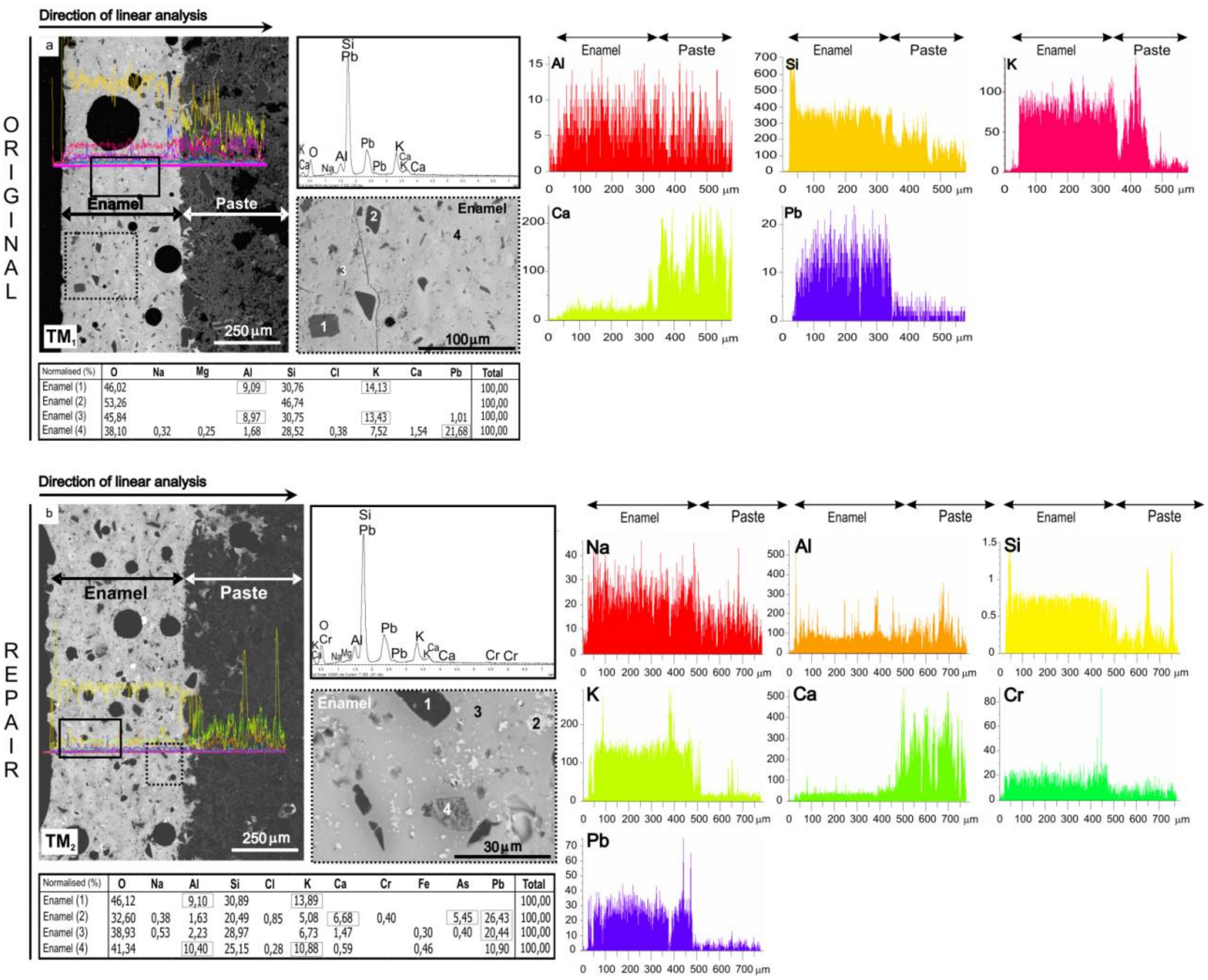

Normalised (%)	O	Na	Mg	Al	Si	Cl	K	Ca	Pb	Total
Enamel (1)	46,02			9,09	30,76		14,13			100,00
Enamel (2)	53,26				46,74					100,00
Enamel (3)	45,84			8,97	30,75		13,43		1,01	100,00
Enamel (4)	38,10	0,32	0,25	1,68	28,52	0,38	7,52	1,54	21,68	100,00

Normalised (%)	O	Na	Al	Si	Cl	K	Ca	Cr	Fe	As	Pb	Total
Enamel (1)	46,12		9,10	30,89		13,89						100,00
Enamel (2)	32,60	0,38	1,63	20,49	0,85	5,08	6,68	0,40		5,45	26,43	100,00
Enamel (3)	38,93	0,53	2,23	28,97		6,73	1,47		0,30	0,40	20,44	100,00
Enamel (4)	41,34		10,40	25,15	0,28	10,88	0,59		0,46		10,90	100,00

The gas bubbles seen are largely generated during firing, a consequence of the release of the gases present in the underlying ceramic paste. Small amounts of CH_4 and NO_x and, to a lesser extent, CO and CO_2, may be released during firing [42]. On occasion, expelling in the kiln the gases housed in the ceramic pastes imbues the material with a spongy texture [43]. The gas bubbles proved to be more abundant in the enamels applied to tiles, made with calcium-rich clays, for when burned calcium carbonate releases CO_2 [44, 45]. The main features observed by means of BSE-SEM in the enamels studied are shown in Table 3. The elements determined with semi-quantitative EDS analyses are shown in Table 4.

CONCLUSIONS

The importance of this study lies primarily in the characterisation of materials used in a protected heritage building and in the experimental data provided on the technology applied to produce them. Clear differences have been established between the original and replacement ceramic materials in both the pastes and enamels studied (experimental data are summarized in Tables 2, 3 and 4). The experimental data provide previously unknown information on the manufacture of these materials, and partially confirmed the reports in the references consulted on the raw materials and reached firing temperatures (information is displayed in Table 5).

The original ceramic cladding contains grog in addition to silica to enhance the strength of the paste. The replacement materials may have been extruded. The repair tiles were deliberately manufactured to be stronger than the original materials, primarily by adding more quartz. The inner fabric wall bricks were insufficiently pressed and fired in uncontrolled atmospheres. The courtyards bricks, by contrast, were carefully manufactured and its strength was raised by adding large amounts of grog.

The ceramic pastes used for the original and replacement tiles as well as the courtyards bricks were made from calcium-rich clay with a certain amount of magnesium. The detection of hematite in the pastes in the original tiles denotes the use of calcium-rich clay which may have also contained iron oxides. The pastes in the original tiles were fired at lower temperatures (>800 °C) than the repair tiles (>>900 °C), which were in turn kilned at lower temperatures than the courtyards bricks (>1000 °C). The mineral paragenesis identified in the courtyards bricks reveals that the technology used raised the temperature to over 1000 °C. The inner fabric wall bricks were made from a mix of kaolinitic and calcitic clays with high iron oxide content and fired at temperatures of over 950 °C.

Lead oxide and silica are the main constituents of the enamel applied to the original ceramic cladding. The high zirconium content might indicate that in the early twentieth century zirconium oxides or silicates were used in place of tin oxide. The bluish hue may have been attained with the addition of vanadium and the glaze applied consisted almost entirely of calcium. The manufacture and application of the enamel coating on the replacement ceramic materials were partially mechanised. Its chlorine and antimony contents should be highlighted. The lead content is lower than in the enamel covering the original cladding and the opacifying capacity afforded by tin may have been partially replaced or reinforced by adding zinc oxides.

The enamel on the original and replacement tiles are found to be fairly similar. A glaze may have been applied to the original enamels. Silicon and lead are the majority elements in both coatings, whose aluminium and potassium contents result particularly significant. The main compositional difference is the presence in the repair tile enamel of particles with high calcium and arsenic contents.

The findings of this research are therefore regarded to constitute a criterion for establishing which of the ceramic materials are original and which replacements. Moreover, the importance of this type of studies for the conservation and/or replacement of materials used in the built heritage is reflected.

ACKNOWLEDGMENTS

The courtesy and support provided by José María la Calle, Deputy General Director of Architecture and Urban Planning of the Community of Madrid, and José María Cabrera, managing director of CPA, S.A., in allowing access to and sampling on the building, are gratefully acknowledged. The authors wish to thank technicians Marián Barajas, Iván Serrano, Eugenio Baldonedo and Alfonso Rodríguez for their assistance. Their gratitude extends to Antonio Perla, Abraham Rubio-Celada, Fernando Agua, Manuel García-Heras and Jesús María Rincón for their valuable knowledge and insightful clarifications. Special thanks are also given to the referees, as its recommendations have improved the paper. This research was funded by the Complutense University of Madrid's research group on the Alteration and conservation of heritage stone (921349), the Geomaterials Programme (P2009/MAT_1629) and CONSOLIDER-TCP (CSD2007-0058).

REFERENCES

[1] Peters T, Iberg R. Mineralogical changes during firing of calcium-rich bricks clays. *Am. Ceram. Soc. Bull.* 1978; **57**(5):503-509.

[2] Heimann RB. Assessing the technology of ancient pottery: the use of ceramic phase diagrams. *Archeomaterials* 1989; **3**:123-148.

[3] Maggetti M. Phase analysis and its significance for technology and origin. In: Olin JS, editor. *Archaeological Ceramics*, Boston: Smithsonian Institution Press; 1982, p. 121-133.

[4] Fort R, Alvarez de Buergo M, López de Azcona C, Mingarro F, Varas MJ, Soriano, J. Caracterización de la Fábrica de Ladrillo del Palacio del Infante Don Luis, Boadilla del Monte, Madrid. *Bol. Soc. Esp. Cerám. Vidrio* 2004;**43**(2):578-582.

[5] Maritan L, Nodari L, Mazzoli C, Milano A, Russo U. Influence of firing conditions on ceramic products: Experimental study on clay rich in organic matter. *Appl. Clay Sci.* 2006;**31**:1-15.

[6] Moropoulou A, Bakolas A, Bisbikou K. Thermal analysis as a method of characterizing ancient ceramic technologies. *Thermoch. Acta* 1995;**2570**:743-753.

[7] Molera J, Pradell T, Vendrell-Saz M. The colours of Ca-rich ceramic pastes: origin and characterization. *Appl. Clay Sci.* 1998;**13**:187-202.

[8] Jordán MM, Boix A, Sanfeliu T, de la Fuente C. Firing transformations of cretaceous clays used in the manufacturing of ceramic tiles. *Appl. Clay Sci.* 1999;**14**(4):225-234.

[9] Riccardi MP, Messiga B, Duminuco P. An approach to the dynamics of clay firing. *Appl. Clay Sci.* 1999;**15**(3-4):393-409.

[10] Cultrone G, Rodriguez-Navarro C, Sebastian E, Cazalla O, de la Torre MJ. Carbonate and silicate phase reactions during ceramic firing. *Eur. J. Mineral.* 2001;**13**:621-634.

[11] Carretero MI, Dondi M, Fabbri B, Raimondo M. The influence of shaping and firing technology on ceramic properties of calcareous and non-calcareous illitic-chloritic clays. *Appl. Clay Sci.* 2002;**20**:301-306.

[12] Trindade MJ, Dias MI, Coroado J, Rocha F. Mineralogical transformations of calcareous rich clays with firing: A comparative study between calcite and dolomite rich clays from Algarve, Portugal. *Appl. Clay Sci.* 2009;**42**:345-355.

[13] Kingery WD, Bowen HK, Uhlmann DR. Introduction to Ceramics. 2nd ed. New York: John Wiley; 1976.

[14] Kingery WD, Vandiever PM. Ceramic Masterpieces. Art, Structure and Technology. New York: The Free Press; 1986.

[15] Rice PM. Pottery analysis. A sourcebook. Chicago: University of Chicago Press; 1987.

[16] Tite MS, Freestone I, Mason R. Lead glazes in antiquity-methods of production and reasons for use. *Archaeometry* 1998;**40**(2):241-260.

[17] Karasu B, Çaki M, Turan S. The development and characterisation of zinc crystal glazes used for Amakusa-like soft porcelains. *J. Eur. Ceram. Soc.*2000;**20**:2225-2231.

[18] Tulyaganov DU, Agathopoulos S, Fernandes HR, Ferreira JMF. The influence of incorporation of ZnO-containing glazes on the properties of hard porcelains. *J. Eur. Ceram. Soc.* 2007;**27**:1665-1670.

[19] Pérez-Monserrat E, Varas MJ, Fort R, Alvarez M. Assessment of Different Methods for Cleaning the Limestone Façades of the Former Workers Hospital of Madrid, Spain. *Stud. Conserv.* 2011;**56**(4):298-313.

[20] Perla A. La Cerámica. In: Un Monumento recuperado: La rehabilitación del Hospital de Jornaleros de Maudes, Madrid. Consejería de Política Territorial, Comunidad de Madrid; 1990, p. 131-161.

[21] Perla A. Antonio Palacios y la cerámica: luz y color en la arquitectura. In: Antonio Palacios, constructor de Madrid. La Librería, Madrid; 2001, p. 289-300.

[22] Rubio-Celada A. De la tradición a la modernidad, los Zuloaga ceramistas. PhD Thesis, Universidad Complutense de Madrid; 2004.

[23] Fazio G, Hreglich S, Lazzarini L, Pirredda L, Verita M. Le Altinelle a Venezia: Problemi Storici, Caratterizzazione Chimico-Fisica, Cause di Deterioramento. In: Il Mattone di Venezia. Contributi Presentati al Concorso di Idee Su Patologia, Diagnosi e Terapia del Mattone di Venezia. Laboratorio Per lo Studio della Dinamica delle Grandi Masse, Venezia; 1982, p.227-291.

[24] Kreimeyer R. Some notes on the firing colour of clay bricks. *Appl. Clay Sci.* 1987;**2**(2):175-183.

[25] Checa A. Evolución del plano de los barrios de Cuatro Caminos y Castillejos. *An. Geog. Univ. Complutense* 1982;**2**:167-180.

[26] Cultrone G, Sebastian E, Elerta K, de la Torre MJ, Cazalla O, Rodriguez-Navarro C. Influence of mineralogy and firing temperature on the porosity of bricks. *J. Eur. Ceram. Soc.* 2004;**24**:547-564.

[27] Segnit ER, Anderson CA. Scanning electron microscopy of fired illite. *Trans. Brit. Ceram. Soc.* 1972;**71**:85-88.

[28] Tite MS, Maniatis Y. Examination of ancient pottery using the scanning electron microscope. *Nature* 1975;**257**(5522):122-123.

[29] López-Arce P, Garcia-Guinea J, Gracia M, Obis J. Bricks in historical buildings of Toledo City: characterisation and restoration. *Mater. Charact.* 2003;**50**:59-68.

[30] López-Arce P, Garcia-Guinea J. Weathering traces in ancient bricks from historic buildings. *Build. Environ.* 2005;**40**:929-941.

[31] Veniale F. Modern techniques of analysis applied to ancient ceramics. In: Advanced workshop on analytical methodologies for the investigation of damaged stones, 1990, Pavia, Italy, 1990.

[32] Flores V, Guiraúm A, Barrios J. Caracterización de ladrillería tradicional producida en la Vega del Guadalquivir, en zonas próximas a Sevilla. *Bol. Soc. Esp. Cerám. Vidrio* 1999;**38**(1):29-34.

[33] Traoré K, Kabre TS, Blanchart P. Low temperature sintering of a clay for pottery from Burkina Faso. *Appl. Clay Sci.* 2000;**17**(5)279-292.

[34] Jordán MM, Sanfeliu T, de la Fuente C. Firing transformations of Tertiary clays used in the manufacturing of ceramic tile bodies. *Appl. Clay Sci.* 2001;**20**:87-95.

[35] Nodari L, Marcuz E, Maritan L, Mazzoli C, Russo U. Hematite nucleation and growth in the firing of carbonate-rich clay for pottery production. *J. Eur. Ceram. Soc.* 2007;**27**:4665-4673.

[36] Maniatis Y, Simopoulos A, Kostikas A. Moessbauer study of the effect of calcium content on iron oxide transformations in fired clays. *J. Am. Ceram. Soc.* 1981;**64**(5):263-269.

[37] González-García F, Romero-Acosta V, García-Ramos G, González-Rodríguez M. Firing transformations of mixtures of clays containing illite, kaolinite and calcium carbonate used by ornamental tile industries. *Appl. Clay Sci.* 1990;**5**(4):361-375.

[38] Traoré K, Kabre TS, Blanchart P. Gehlenite and anorthite crystallisation from kaolinite and calcite mix. *Ceram. Int.* 2003;**29**:377-383.

[39] Vielhaber L. Tecnología de los esmaltes. Madrid: Ed. Reverté; 1954.

[40] Rincón JM, Márquez H, Rivera E. Electron microscopy and EDX microanalysis of photochromic silver halide glasses of the composition systems: Al_2O_3-B_2O_3-SiO_2 and Na_2O-CaO-SiO_2. *J. Mat. Sci.* 1991;**26**:1192-1198.

[41] Díaz C, Torres-Martínez LM, Garza L, Avalos M, Rincón JM. Turning geothermal waste into glasses and glass-ceramics. *Amer.Cer.Soc.Bull.* 1993;**72**(10):81-82.

[42] Toledo R, dos Santos DR, Faria Jr RT, Carrio JG, Auler LT, Vargas H. Gas release during clay firing and evolution of ceramic properties. *Appl. Clay Sci.* 2004;**27**:151-157.

[43] Freestone IC, Middleton AP. Mineralogical applications of the analytical SEM in archaeology. *Mineral. Mag.* 1987;**51**:21-31.

[44] Rincón JM, Romero M. Basis and classification of efflorescences in construction bricks. *Mater. Construcc.* 2000;**50**(260):63-69.

[45] Jordán MM, Almendro-Candel MB, Romero M, Rincón JM. Application of sewage sludge in the manufacturing of ceramic tile bodies. *Appl. Clay Sci.* 2005;**30**:219-224.

Figure captions

Fig. 1. Decorative ceramic materials currently adorning façades and central garden fountain in the Former Workers Hospital of Maudes (Madrid, Spain).

a. Decorative ceramic cladding on façades, installed ca 1986.
b. Original ceramic cladding on the section of the fountain.
c. Fountain: tile mosaic covering the interior of the basin.
d. Mosaic in basin of fountain: (1) original and (2) repaired (ca 1986).

Fig. 2. Plan view of building showing location of ceramic materials studied.

Decorative ceramics: original and replacement cladding (CC_1 and CC_2) and original and repair tile mosaic (TM_1 and TM_2); original structural bricks: inner fabric walls (FB) and courtyards (CB).

Fig. 3. Naked eye views and polarised optical microscopic micrographs of ceramic materials studied. The higher luminosity micrographs have been taken with plane-polarized light and the darker ones with cross- polarized light.

Fig. 4. X-ray diffraction patterns for ceramic pastes studied (Qtz: quartz; Kfs: potassium feldspar; P: phyllosilicates; Hem: hematite; Wo: wollastonite; Di: diopside; Gh: gehlenite; An: anorthite).

Fig. 5. Backscattered mode scanning electron microscopy (BSE-SEM) micrographs and energy dispersive X-ray spectra (EDS) of the enamels applied to original and replacement ceramic cladding.

Fig. 6. Backscattered mode scanning electron microscopy (BSE-SEM) micrographs and energy dispersive X-ray spectra (EDS) of the enamels applied to original and repair mosaic tiles.

Tables

Type of ceramic material			Date	Location	Denomination	Characterisation techniques
DECORATIVE CERAMICS	Ceramic cladding	Ceramic paste + enamel	1914 (original)	Section fontaine, central garden	CC$_1$	Spectrophotometry, POM, XRD, SEM-EDS
			±1985 (replacement)	SE bay	CC$_2$	Spectrophotometry, POM, XRD, SEM-EDS
	Tile mosaic	Ceramic paste + enamel	1914 (original)	Fountain basin, central garden	TM$_1$	Spectrophotometry, POM, XRD, SEM-EDS
			±1985 (repair)	Fountain basin, central garden	TM$_2$	Spectrophotometry, POM, XRD, SEM-EDS
STRUCTURAL BRICKS		Ceramic paste	±1909 -1910 (original)	Inner fabric wall, church	FB	Spectrophotometry, POM, XRD
			±1914 -1916 (original)	Courtyard, SW bay	CB	Spectrophotometry, POM, XRD

Table 1. Ceramic materials studied (decorative ceramics and structural bricks) and characterisation techniques used.

CERAMIC PASTE		CIELab	Petrographic analysis (POM)				Mineralogical characterisation (XRD)							
			a:p	Clay pellets	Opaque minerals	Grog	Qtz	Kfs	P	Hem	Wo	Di	Gh	An
Ceramic cladding	Original (CC$_1$)	L*=67.42 a*=13.83 b*=21.75	3:1	Yes	Yes	Yes	X							
	Replacement (CC$_2$)	L*=66.58 a*=20.69 b*=27.06	3:1	No	Yes	No	X		X					
Tile mosaic	Original (TM$_1$)	L*=73.27 a*=9.90 b*=20.21	1:3	No	No	No	X	X		X	X	X	X	X
	Repair (TM$_2$)	L*=75.85 a*=5.44 b*=23.18	3:1	No	No	No	X			X	X	X	X	
Structural bricks (original)	Inner fabric wall (FB)	See text	1:2	No	No	No	X	X		X			X	X
	Courtyards (CB)	L*=72.97 a*=9.00 b*=26.51	1:4	No	No	Sí	X	X			X	X	X	X

Table 2. Colour parameters, main petrographic features and mineralogical identification for ceramic pastes.
(a:p: aggregate:paste; Qtz: quartz; Kfs: potassium feldspar; P: phyllosilicates; Hem: hematite; Wo: wollastonite; Di: diopside; Gh: gehlenite; An: anorthite)

ENAMELS		Hue	CIELab	Petrographic analysis (POM) and scanning electron microscopic (BSE-SEM) description					
				Thickness	Enamel-ceramic paste contact	Gas bubbles	Glaze*	Glaze**	Other
Ceramic cladding	Original (CC$_1$)	Bluish	L*=63.09 a*=-10.18 b*=-3.18	±constat 200 μm	Continuous Irregular	Yes 100 μm	Applied	Observed Thickness ±20 μm Made of Ca	Uneven Handmade
	Replacement (CC$_2$)	Bluish-green	L*=56.38 a*=-19.75 b*=-3.46	Constat 500 μm	Smooth Continuous Regular	No	Applied	Not observed	Even Semi-industrial application
Tile mosaic	Original (TM$_1$)	Greenish-blue	L*=61.36 a*=-11.30 b*=-3.03	Constat 330 μm	Continuous Irregular	Yes Up to 150 μm	Not applied	Observed under POM	Uneven Abundant Q
	Repair (TM$_2$)	Green	L*=52.56 a*=-14.95 b*=17.39	Constat 450 μm	Straight ±irregular	Yes 25-90 μm	Not applied	Not observed	Uneven Abundant Q

Table 3. Chromatic parameters determined and main features observed in the enamels studied by polarised optical and scanning electron microscopy.
* According to information on glazing reported in the literature consulted.
** According to data on glazing provided by experimental characterisation.

ENAMELS		**Constituent elements detected with semi-quantitative EDS analyses**																		
		Na	**Mg**	**Al**	**Si**	**S**	**Cl**	**K**	**Ca**	**Ti**	**V**	**Cr**	**Fe**	**Cu**	**Zn**	**As**	**Zr**	**Sn**	**Sb**	**Pb**
Ceramic cladding	Original (CC_1)			x	**X**			x		x	x		x				**X**			**X**
	Replacement (CC_2)	x		x	**X**	x	x	x	x				x	x	x			**X**	x	**X**
Tile mosaic	Original (TM_1)	x		**X**	**X**			**X**	x											**X**
	Repair (TM_2)	x	x	**X**	**X**			**X**	x			x				x				**X**

Table 4. Elements identified by SEM-EDS in enamels analysed (capitalised bold X indicates the most abundant element in each sample).

CERAMIC PASTES		**References consulted**				**Characterisation results**			
		Ceramic artist, Location	**Raw materials**		**Manufacture**	**Clay materials**	**Additives**	**Firing temperature**	**Manufacture**
			Clays	**Additives**					
Ceramic cladding	Original (CC_1)	Zuloaga, Segovia 1914	Segovian OxFe-rich red clay	Abundant Segovian silica	Pinewood kiln Oxidising atm. 1200 °C	Red clays	Abundant quartz and *grog*	Not over 1100; 1200 °C not ruled out	*Incomplete mixing (clay pellets* Hand made
	Replace-ment (CC_2)	Madrid ±1985	Madrilenian clay	Segovian soil, quartz and grog from Teruel	Electrical kiln Oxidising atm. Semi-mechanic. 1200-1250 °C	Clays	Abundant quartz	Reference reports unconfirmed	*Completely mixed* *Semi-industrial* *Paste extrusion*
Tile mosaic	Original (TM_1)	Ramos Rejano, Seville ±1915	No data	No data	No data	*Ca-rich clay (and/or some Mg) and FeOx*	*Scant quartz*	*Gh >Di, Wo & An > 800 ℃*	
	Repair (TM_2)	Ceramics School Madrid ±1985	Red mud	Ca-rich pastes and Madrid sand	1030 °C	*Clay with less Ca (and/or some Mg)* *Si_2O* and FeOx	Abundant quartz	*Gh ≈ Di & Wo >>900 ℃*	*Stronger pastes than in original tiles*
Structural bricks (original)	Inner fabric wall (FB)	No data				*Mix of FeOx-rich kaolinitic clays and calcitic*	*Quartz*	*Gh & An >950 ℃*	*Scantly pressed* *Uncontrolled atm* *Neabyr brickwork* *Hand made*
	Courtyards (CB)	No data				*Ca-rich clay (and/or some Mg)*	*Very abun-dant grog*	*Gh < Di, Wo & An > 1000 ℃*	*Meticulous* *Highly mechan-ised*

Table 5. Summary of information from literature and from the characterisation carried out (in italics). All locations are in Spain.